

Molecular Meccano, 48^{l±l} Probing Co-Conformational Changes in Chiral [2]Rotaxanes by ¹H-NMR Spectroscopy

Peter R. Ashton,^[a] José A. Bravo,^[b] Francisco M. Raymo,^[b] J. Fraser Stoddart,^{*,[b]}
Andrew J. P. White,^[c] and David J. Williams^{*,[c]}

Keywords: Co-conformation / Molecular recognition / Planar chirality / Rotaxanes / Template-directed synthesis

The template-directed syntheses of three [2]rotaxanes possessing either chiral centers or elements of planar chirality, in one of their two mechanically interlocked components, have been realized and their solid-state structures have been analyzed by X-ray crystallography. In one instance, an enantiomerically pure dumbbell-shaped component incorporating a 1,5-dioxynaphthalene recognition site and two (1*R*,2*S*,5*R*)-menthyl stoppers was employed to template the formation of the achiral tetracationic cyclophane, cyclobis(paraquat-*p*-phenylene). The resulting enantiomerically pure [2]rotaxane was isolated in a yield of 55%. In the other two instances, an achiral 1,5-dioxynaphthalene-based dumbbell-shaped component was employed to template the formation of bipyridinium-based

cyclophanes possessing either one or two elements of planar chirality. The resulting [2]rotaxane, possessing *one* element of planar chirality, was isolated as a racemate in a yield of 24%. The related [2]rotaxane, possessing *two* elements of planar chirality, was isolated as a mixture of a *meso* form and an enantiomeric pair in an overall yield of 28%. The ¹H-NMR-spectroscopic analysis of this mixture revealed a diastereoisomeric ratio of 4:1. A degenerate co-conformational change was identified by variable-temperature ¹H-NMR spectroscopy in all [2]rotaxanes. The symmetry loss arising from the introduction of one or two elements of planar chirality enabled the elucidation of the mechanism of this dynamic process in two instances.

Introduction

The tetracationic cyclophane, cyclobis(paraquat-*p*-phenylene), binds^[1] 1,5-dioxynaphthalene-based acyclic polyethers in a pseudorotaxane manner in both solution and the solid state. [C–H···O] Hydrogen bonds between the α -bipyridinium protons and the polyether oxygen atoms, [π ··· π] stacking between the complementary aromatic units, and [C–H··· π] interactions between the 1,5-dioxynaphthalene protons ($H_{4/8}$) and the *p*-phenylene rings are responsible for the formation of these supramolecular complexes. This molecular recognition motif suggested to us the design of template-directed^[2] synthetic approaches to rotaxanes.^[3] Indeed, the kinetically controlled self-assembly^[4] of [2]rotaxanes, incorporating cyclobis(paraquat-*p*-phenylene) and a 1,5-dioxynaphthalene-based dumbbell-shaped component, has been realized^[5] in very high yields by allowing appropriate acyclic precursors of the tetracationic cyclophane component to react in the presence of a preformed dumbbell-shaped template. In solution, three degenerate dynamic processes can be envisaged in these [2]rot-

axanes, as suggested by variable-temperature ¹H-NMR spectroscopy. However, as a result of the high degree of symmetry possessed by these mechanically interlocked molecules, it was not possible to establish if one, two, or all three processes are indeed occurring in solution. In order to gain further insight into the nature of these degenerate co-conformational^[6] changes and intrigued by the possibility of extending these template-directed approaches to the synthesis of chiral rotaxanes,^{[7][8]} we envisaged the prospect of introducing either chiral centers or elements of planar chirality^[9] into the dumbbell-shaped or tetracationic cyclophane components, respectively. Here, we report (i) the template-directed syntheses of a [2]rotaxane incorporating several chiral centers in the stoppers, as well as of two [2]rotaxanes, one incorporating one element and the other two elements of planar chirality within their tetracationic cyclophane component, (ii) the ¹H-NMR-spectroscopic investigation of the degenerate dynamic processes associated with co-conformational changes in these [2]rotaxanes in solution, and (iii) their X-ray crystallographic analyses in all three cases.

Results and Discussion

Synthesis

Alkylation of **1** with BrCH₂CO₂tBu afforded **2** (Scheme 1), which was treated with CF₃CO₂H to yield **3**. The bis(carboxylic acid) **3** was converted into the corresponding bis(acid chloride), which was allowed to react with

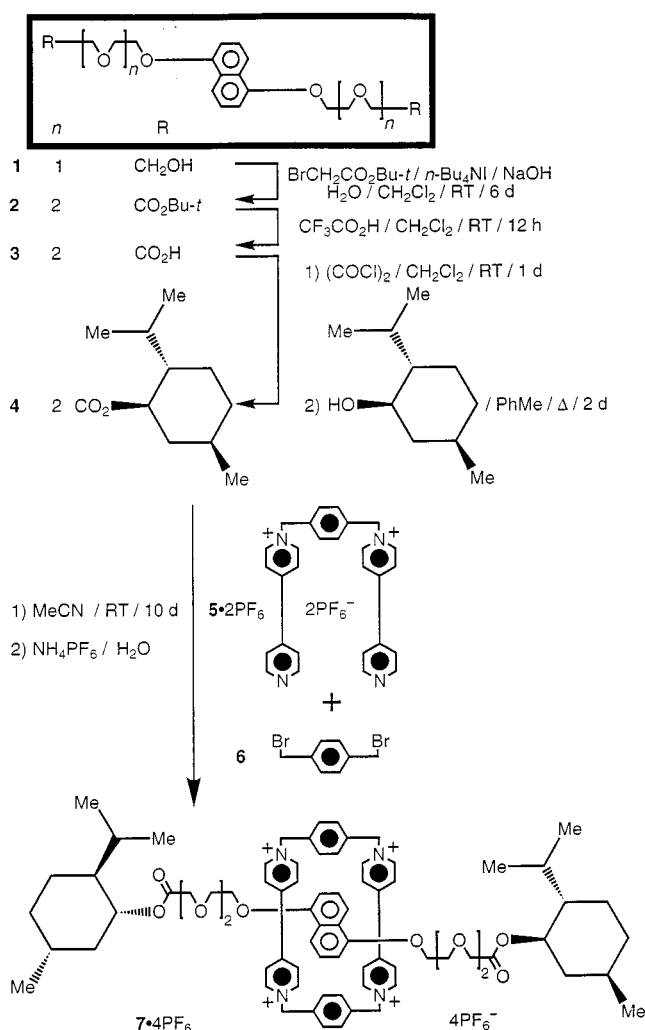
[[±]] Part 47: K. N. Houk, S. Menzer, S. P. Newton, F. M. Raymo, J. F. Stoddart, D. J. Williams, *J. Am. Chem. Soc.*, in press.

[^a] School of Chemistry, University of Birmingham, Edgbaston, Birmingham, B15 2TT, UK

[^b] Department of Chemistry and Biochemistry, University of California, Los Angeles, 405 Hilgard Avenue, Los Angeles, CA 90095-1569, USA
Fax: (internat.) + 1-310/206-1843
E-mail: stoddart@chem.ucla.edu

[^c] Department of Chemistry, Imperial College, South Kensington, London, SW7 2AY, UK
Fax: (internat.) + 44-171/594-5835

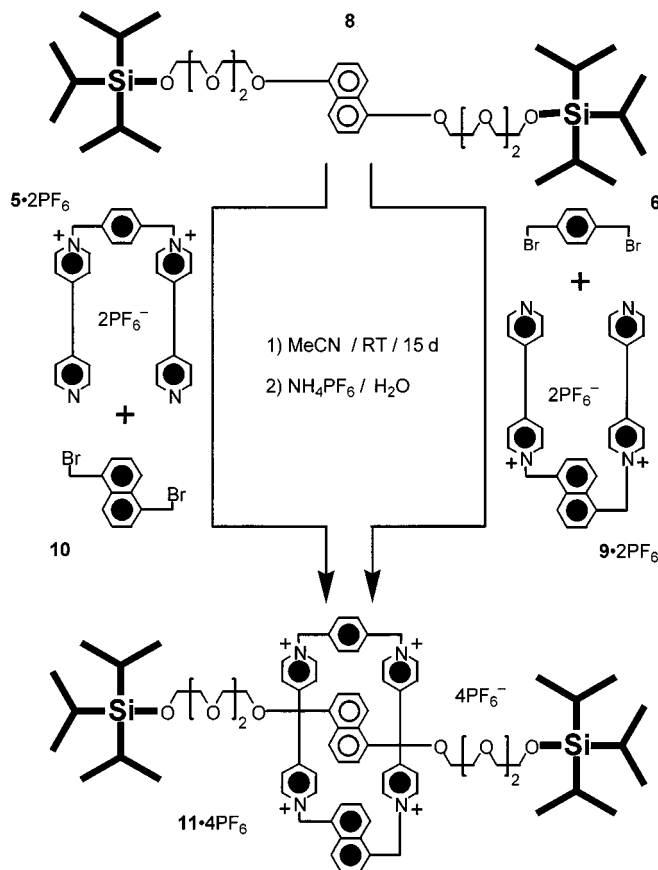
(1*R*,2*S*,5*R*)-menthol to afford the chiral dumbbell-shaped compound **4**. Reaction of **5** · 2 PF₆ and **6** in the presence of **4** gave the chiral [2]rotaxane **7** · 4 PF₆ after counterion exchange. The [2]rotaxane **11** · 4 PF₆ was obtained as a racemic modification from achiral precursors after the reaction of either **5** · 2 PF₆ and **10** or **6** and **9** · 2 PF₆ in the presence of **8** (Scheme 2), followed by counterion exchange. Similarly, the [2]rotaxane **12** · 4 PF₆ was prepared as a mixture of a *meso* form and one pair of enantiomers from achiral precursors after the reaction of **9** · 2 PF₆ and **10** (Scheme 3). The tetracationic cyclophane **14** · 4 PF₆ was obtained as a racemate from achiral precursors by allowing **5** · 2 PF₆ to react with **10** in the presence of **13** (Scheme 4).



Scheme 1. Template-directed synthesis of the [2]rotaxane **7** · 4 PF₆.

X-Ray Crystallography

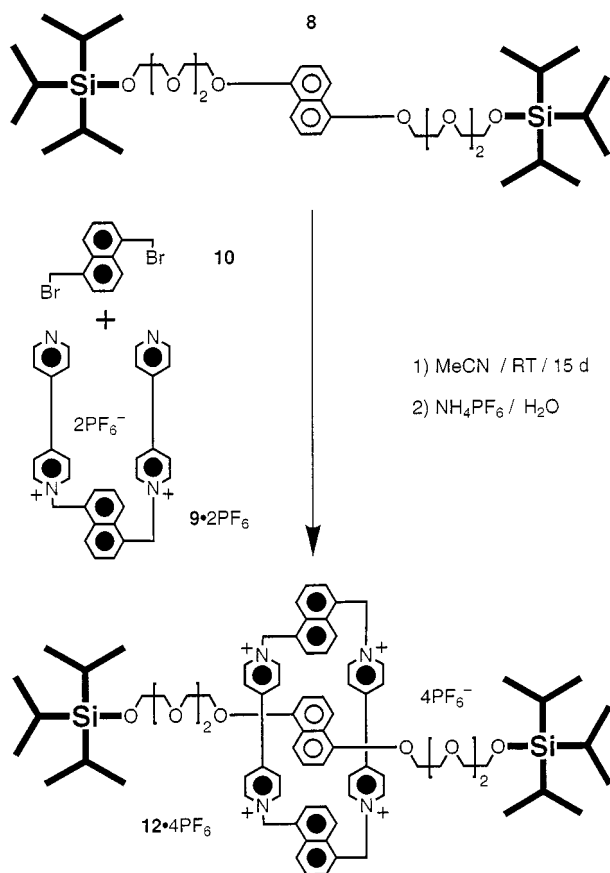
The X-ray analysis of **7** · 4 PF₆ showed the crystals to contain two crystallographically independent [2]rotaxanes (**a** and **b**) in the asymmetric unit (Figure 1). In both cases, the 1,5-dioxynaphthalene ring system of the dumbbell-shaped component is sandwiched symmetrically between the two bipyrindinium units of the tetracationic cyclophane



Scheme 2. Template-directed synthesis of the [2]rotaxane **11** · 4 PF₆.

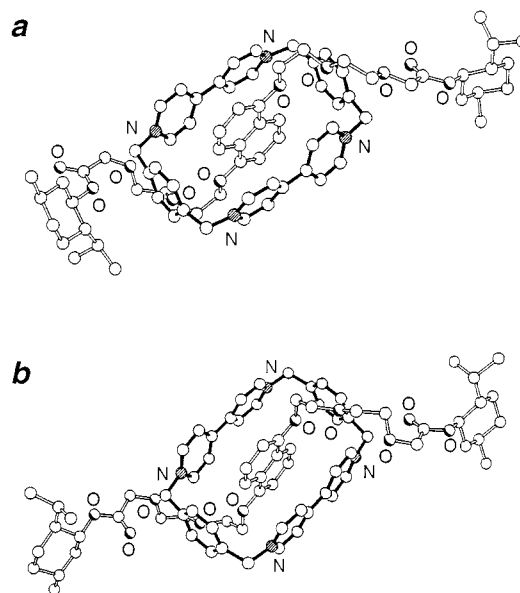
– π - π separations in the range 3.37–3.42 Å. Additional stabilization occurs via [C–H $\cdots\pi$] interactions between the *peri*-hydrogen atoms of the 1,5-dioxynaphthalene ring systems and the *p*-xylyl spacer in the cyclophane – [H $\cdots\pi$] distances are in the range 2.52–2.59 Å with [C–H $\cdots\pi$] angles of 151–159°. In **a**, these aryl–aryl interactions are supplemented by [C–H \cdots O] hydrogen bonds between α -bipyridinium hydrogen atoms and either the second or third oxygen atoms in the polyether chains – [H \cdots O] distances are in the range 2.30–2.40 Å with associated [C–H \cdots O] angles of 129–154°. In **b**, there are analogous [H \cdots O] interactions with [H \cdots O] distances of 2.24–2.49 Å and with [C–H \cdots O] angles of 116–159°. Here, these interactions are further supplemented by [C–H \cdots O] hydrogen bonds from methylene hydrogen atoms in the cyclophane and the carbonyl oxygen atoms of the ester functions in the dumbbell-shaped component – [H \cdots O] distances of 2.28–2.45 Å and with [C–H \cdots O] angles of 161–162°. There are no intermolecular contacts of note.

A crystallographic study of the complex formed between the thread **13** – used to template the synthesis of the tetracationic cyclophane **14** · 4 PF₆ (Scheme 4) – showed the crystals to contain two independent [2]pseudorotaxanes, together with an additional uncomplexed molecule of **13**. The gross superstructure suffers from extensive disorder, partly as a consequence of crystallographically imposed inversion symmetry to the tetracationic cyclophane component (that

Scheme 3. Template-directed synthesis of the [2]rotaxane $12 \cdot 4 \text{PF}_6$

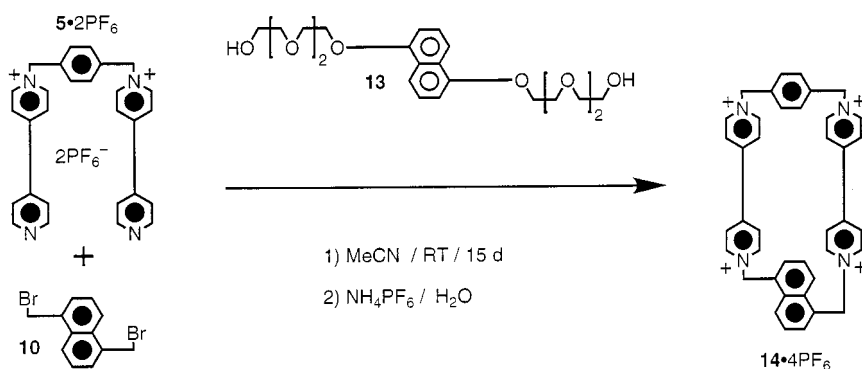
results in superimposition of the *p*-xylyl and 1,5-disubstituted naphthalene ring systems) and partly on account of the adoption of several conformations by the polyether chains. Because of these problems, detailed refinement of the gross superstructure proved impracticable and the only definitive features to emerge are the 3:2 stoichiometry of **13** to **14** · 4 PF_6 and the sandwiching of the 1,5-dioxynaphthalene ring system between bipyridinium units in the [2]pseudorotaxanes.

The [2]rotaxane **11** · 4 PF_6 also has a disordered structure in the solid state on account of crystallographically imposed inversion symmetry. Figure 2 depicts one of several co-conformations present in the crystals. In this structure, the dis-

Figure 1. Ball-and-stick representations of the two crystallographically independent structures **a** and **b** associated with the [2]rotaxane 7^{4+} in the solid state

ordered has been resolved and has been shown to be associated in part with the center of the 1,5-dioxynaphthalene ring system being displaced by ca. 0.6 Å from the crystallographic inversion center in the plane of the ring system. As a consequence, there are also two partially overlapping conformations of the polyether chains present, thus rendering detailed analysis of intracomplex interactions unrealistic. The only hydrogen-bonding interaction involving ordered components of the [2]rotaxane are between α -bipyridinium hydrogen atoms in the cyclophane and the third oxygen atom in the polyether chains – the $[\text{C} \cdots \text{O}]$ distances are 3.34 Å. There are no intermolecular π -stacking interactions.

X-ray analysis of crystals of the [2]rotaxane **12** · 4 PF_6 yet again revealed a symmetry-imposed disordered structure (Figure 3), although here the disorder is confined to the tetracationic cyclophane component and can be visualized as reflecting a pedalling motion of the two 1,5-disubstituted naphthalene ring systems.^[10] The 1,5-dioxynaphthalene ring system of the dumbbell-shaped compo-

Scheme 4. Template-directed synthesis of the tetracationic cyclophane $14 \cdot 4 \text{PF}_6$

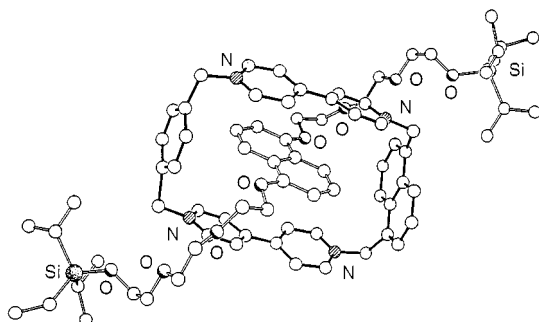


Figure 2. Ball-and-stick representation of structure adopted by the [2]rotaxane **11**⁴⁺ in the solid state

nent is sandwiched symmetrically between the two bipyridinium units of the cyclophane with a mean π - π separation 3.49 Å. Additional stabilization is via bifurcated [C-H \cdots O] hydrogen bonds between α -bipyridinium hydrogen atoms and the second and third oxygen atoms of the polyether chains – the [H \cdots O] distances are 2.40 and 2.47 Å with [C-H \cdots O] angles of 153 and 127°, respectively. There is an absence of any intermolecular π - π stacking interactions.

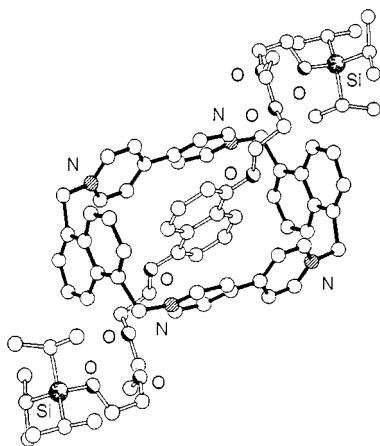


Figure 3. Ball-and-stick representation of structure adopted by the [2]rotaxane **12**⁴⁺ in the solid state

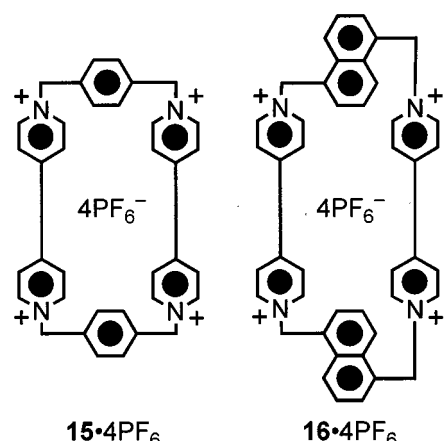
¹H-NMR Spectroscopy

Comparison of the ¹H-NMR spectra (CD₃CN, 298 K) of the dumbbell-shaped compound **4** and of the [2]rotaxane **7** · 4 PF₆ shows significant chemical shift changes for the resonances associated with the 1,5-dioxynaphthalene ring protons (Table 1). The difference is particularly evident for the signals associated with H^{4/8} which shift upfield ($\Delta\delta = -5.34$) and appear at $\delta = 2.46$ in the case of the [2]rotaxane. This dramatic change is a result of shielding effects exerted by the sandwiching bipyridinium units. The ¹H-NMR spectrum (CD₃CN, 298 K) of the free tetracationic cyclophane **15** · 4 PF₆ reveals two sets of signals for the bipyridinium protons (Table 1). In the [2]rotaxane **7** · 4 PF₆, the local C₂ symmetry of the 1,5-dioxynaphthalene unit and the presence of chiral centers in the stoppers give rise to four different environments (sites A–D) for the α -bipyridi-

nium protons H¹_a–H⁸_a (Figures 4–6). The exchange of protons H¹_a–H⁸_a between sites A–D can occur as the result of the degenerate dynamic processes illustrated in Figures 4–6. Process I (Figure 4) involves (i) the dislodgment of the 1,5-dioxynaphthalene unit from the cavity of the tetracationic cyclophane, followed by (ii) a 180° rotation around the axis of its central carbon–carbon bond, and then (iii) its re-insertion inside the cavity of the tetracationic cyclophane. Process II (Figure 5) involves (i) the dislodgment of the 1,5-dioxynaphthalene ring system from the cavity of the tetracationic cyclophane, followed by (ii) a 180° rotation of the tetracationic cyclophane around an axis passing through its center of inversion and perpendicular to its mean plane (defined by the four methylene carbon atoms), and then (iii) the re-insertion of the 1,5-dioxynaphthalene ring system inside the cavity of the tetracationic cyclophane. Process III (Figure 6) involves (i) the dislodgment of the 1,5-dioxynaphthalene ring system from the cavity of the tetracationic cyclophane, followed by (ii) a 180° rotation of one of the bipyridinium units around its [N \cdots N] axis, and then (iii) re-insertion of the 1,5-dioxynaphthalene ring system inside the cavity of the tetracationic cyclophane. When all three of these dynamic processes are slow on the ¹H-NMR timescale, four sets of resonances are expected for protons H¹_a–H⁸_a in the ¹H-NMR spectrum. When one process is fast and two are slow, protons H¹_a–H⁸_a should give rise to two sets of signals. When all three dynamic processes are fast, only one set of signals is expected for protons H¹_a–H⁸_a. It transpires that, at 200 K in (CD₃)₂CO, all three processes are slow. Four sets of resonances, two of which are isochronous, are observed for protons H¹_a–H⁸_a (Figure 7a). At 298 K in CD₃CN, one of the three dynamic processes becomes fast and protons H¹_a–H⁸_a resonate as two sets of signals (Table 1 and Figure 7b). Upon warming the CD₃CN solution up, the two sets of resonances coalesce into one as two, if not all three dynamic processes, are now fast (Figures 7c–7e). By employing the approximate coalescence method,^[11] the kinetic parameters associated with the degenerate site-exchange processes were determined (Table 2).^[12]

In the [2]rotaxane **11** · 4 PF₆, the local C_{2h} symmetry of the 1,5-dioxynaphthalene ring system and the local C₂ symmetry of the 1,5-disubstituted naphthalene spacer of the tetracationic cyclophane impose (Figure 5) four different environments (sites E–H) on the pairs of protons H¹_g–H⁴_g on the methylene groups adjacent to the naphthalene spacer of the tetracationic cyclophane. The exchange of protons H¹_g and H⁴_g between sites E and H, as well as the exchange of protons H²_g and H³_g between sites F and G, occur as a result of processes similar to I and/or II in Figures 4 and 5. By contrast, the process similar to III in Figure 6 has no influence on the environments (sites E–H) associated with the protons H¹_g–H⁴_g. Exchanges of protons H¹_g and H³_g between sites E and G, as well as of protons H²_g and H⁴_g between sites F and H, occur as a result of a new process, namely IV (Figure 8) which involves (i) the dislodgment of the 1,5-dioxynaphthalene ring system from the cavity of the tetracationic cyclophane, followed by

Table 1. Chemical-shift values^[a] for the bipyridinium and the 1,5-dioxynaphthalene protons of **4**, **7** · 4 PF₆, **8**, **11** · 4 PF₆, **12** · 4 PF₆, **14** · 4 PF₆, **15** · 4 PF₆, and **16** · 4 PF₆



Compound	H _a ^[b]	H _β ^[c]	H ^{2/6} ^[d]	H ^{3/7} ^[e]	H ^{4/8} ^[f]
4	—	—	6.77	7.27	7.80
7 · 4 PF ₆	9.04/8.64	7.41/7.23	6.27	6.04	2.46
8	—	—	6.92	7.36	7.78
11 · 4 PF ₆	8.79	7.26	6.14	4.14	2.63
12 · 4 PF ₆	8.70	7.17	6.50	3.27	2.66/2.48 ^[g]
14 · 4 PF ₆	8.92/8.84	8.08	—	—	—
15 · 4 PF ₆	8.89	8.17	—	—	—
16 · 4 PF ₆	8.90	8.00	—	—	—

^[a] The chemical shift values (δ , ppm) reported correspond to the center of each set of signals associated with the protons listed and were determined in CD₃CN at 298 K for **4**, **7** · 4 PF₆, **8**, **14** · 4 PF₆, **15** · 4 PF₆, and **16** · 4 PF₆ and at 353 K for **11** · 4 PF₆ and **12** · 4 PF₆. — ^[b] Hydrogen atoms in the α -positions, with respect to the nitrogen atoms, on the bipyridinium units. — ^[c] Hydrogen atoms in the β -positions, with respect to the nitrogen atoms, on the bipyridinium units. — ^[d] Hydrogen atoms in the positions 2 and 6 on the 1,5-dioxynaphthalene unit. — ^[e] Hydrogen atoms in the positions 3 and 7 on the 1,5-dioxynaphthalene unit. — ^[f] Hydrogen atoms in the positions 4 and 8 on the 1,5-dioxynaphthalene unit. — ^[g] The [2]rotaxane **12** · 4 PF₆ exists as a mixture of a *meso* form and a pair of enantiomers: As a result, two sets of signals are observed for the protons H^{4/8}.

(ii) a 180° rotation of the 1,5-disubstituted naphthalene spacer in the tetracationic cyclophane around the axis of its central carbon–carbon bond, and (iii) the re-insertion of the 1,5-dioxynaphthalene ring system inside the cavity of the tetracationic cyclophane. The inversion of the two enantiomers [(*S*) and (*R*)] of the [2]rotaxane **11** · 4 PF₆ occurs as a result of process IV. When processes I, II, and IV are slow on the ¹H-NMR timescale, four sets of signals are expected for protons H_g¹–H_g⁴ in the ¹H-NMR spectrum of the [2]rotaxane. When processes I and/or II or IV are fast, two sets of resonances should be observed. When processes I and/or II and IV are fast, only one signal is expected. The ¹H-NMR spectrum (CD₃CN, 243 K) of **11** · 4 PF₆ shows two AB systems for protons H_g¹–H_g⁴, as well as six sets of resonances for the 1,5-dioxynaphthalene protons (Figure 9a). These observations indicate that processes I, II, and IV are slow on the ¹H-NMR timescale at this temperature. Upon warming the solution up, only one AB system is observed for protons H_g¹–H_g⁴, suggesting that processes I

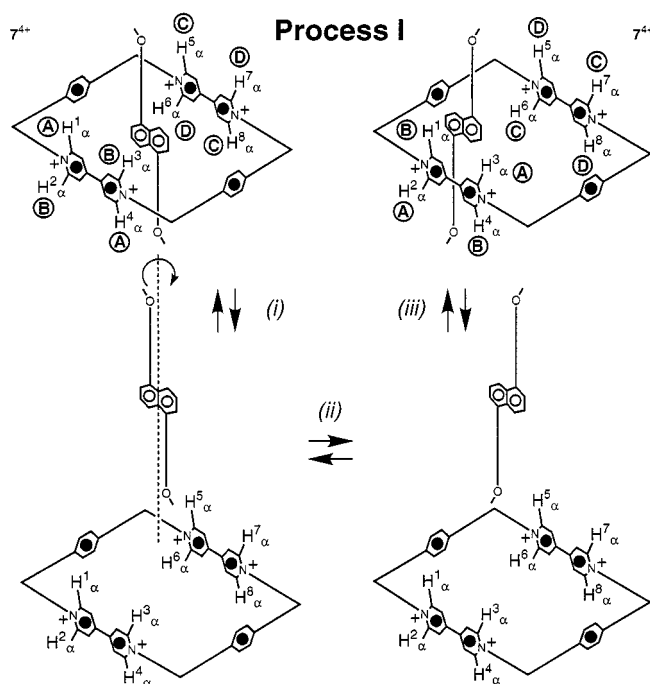


Figure 4. The degenerate site-exchange process I associated with the [2]rotaxane **7** · 4 PF₆ in solution; A–D indicate the different environments imposed on the bipyridinium protons H^{1a}–H^{8a} by the local C₂ symmetry of the 1,5-dioxynaphthalene unit

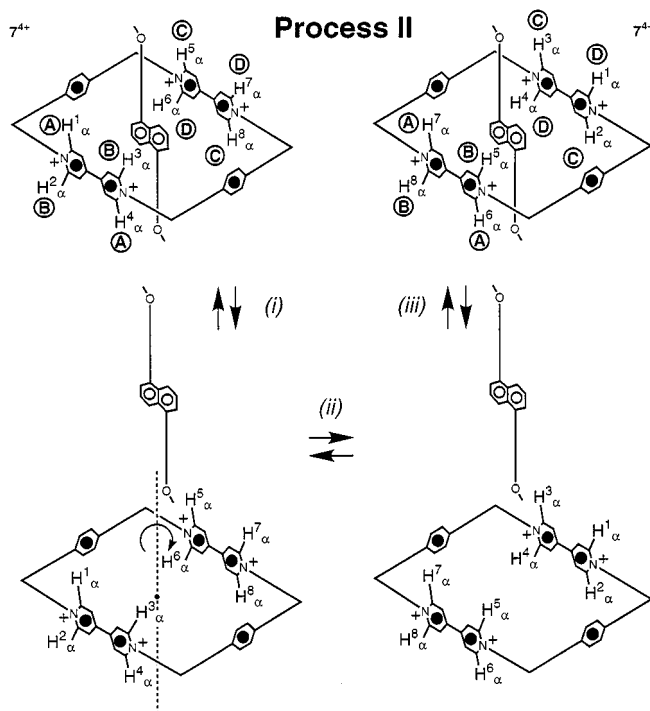


Figure 5. The degenerate site-exchange process II associated with the [2]rotaxane **7** · 4 PF₆ in solution; A–D indicate the different environments imposed on the bipyridinium protons H^{1a}–H^{8a} by the local C₂ symmetry of the 1,5-dioxynaphthalene unit

and/or II or IV are now fast on the ¹H-NMR timescale (Figure 9b). The fact that only three sets of resonances can now be observed for the 1,5-dioxynaphthalene protons indicates that processes I and/or II are fast, while process IV is

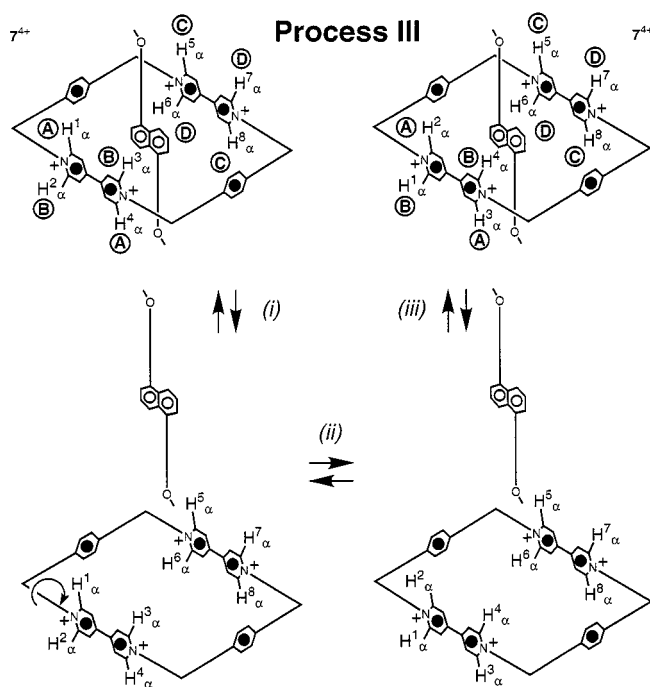


Figure 6. The degenerate site exchange process **III** associated with the [2]rotaxane **7** · 4 PF₆ in solution; A–D indicate the different environments imposed on the bipyrindinium protons H¹_a–H⁸_a by the local C₂ symmetry of the 1,5-dioxynaphthalene unit

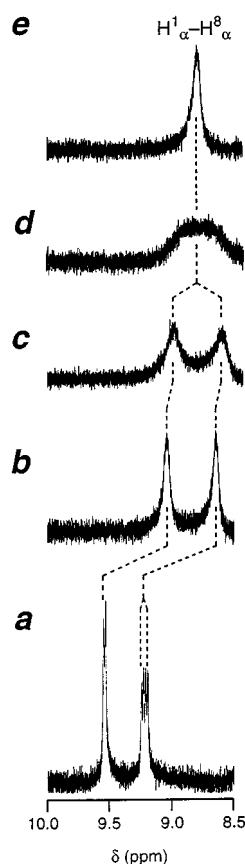


Figure 7. Partial ¹H-NMR spectra of the [2]rotaxane of **7** · 4 PF₆ recorded in (CD₃)₂CO at (a) 200 K and in CD₃CN at (b) 298, (c) 310, (d) 320, and (e) 340 K

slow. By employing the approximate coalescence treatment and protons H¹_g–H⁴_g as probes, the free energy barrier associated with the degenerate site exchange process was determined^[13] (Table 2). Interestingly, protons H¹_g–H⁴_g resonate as a single AB system, even at 353 K, indicating that process **IV** is still slow on the ¹H-NMR timescale.^[14]

The [2]rotaxane **12** · 4 PF₆ exists as a mixture of the *meso* form (*SR*) or (*RS*) and the two enantiomers (*SS*) and (*RR*) which are expected to interconvert as a result of process **IV** (Figure 10). However, in the ¹H-NMR spectrum (CD₃CN, 353 K) of **12** · 4 PF₆, the 1,5-dioxynaphthalene protons H⁴/₈ give rise to two sharp and well-resolved sets of signals at δ = 2.66 and 2.48 in a ratio of 1:4 (Table 1). These observations indicate that the interconversions between the three forms of **12** · 4 PF₆ are slow, or indeed are not occurring at all on the ¹H-NMR timescale at this temperature.^[14] The local C_{2h} symmetry of the 1,5-dioxynaphthalene unit imposes two different environments (sites **I** and **J**) on protons H¹_d and H²_d attached to positions 2 and 6 of the 1,5-disubstituted naphthalene spacers in the tetracationic cyclophane and also imposes two different environments (sites **K** and **L**) on protons H¹_e and H²_e attached to positions 3 and 7 of the same unit (Figure 11). Exchange of protons H¹_d and H²_d between sites **I** and **J**, as well as of protons H¹_e and H²_e between sites **K** and **L**, can occur as a result of processes **I**, **II**, and/or **IV** (Figure 11).^[15] By contrast, the process similar to **III** in Figure 6 has no influence on the environments (sites **I**–**L**) associated with protons H¹_d, H²_d, H¹_e, and H²_e. The ¹H-NMR spectrum [(CD₃)₂CO, 213 K] of the [2]rotaxane **12** · 4 PF₆ shows two sets of signals for protons H¹_d and H²_d and two sets of signals for protons H¹_e and H²_e indicating that processes **I**, **II**, and **IV** are slow on the ¹H-NMR timescale at this temperature (Figure 12a). Upon warming the solution up, process(es) **I** and/or **II** become faster and the two sets of resonances observed for the protons H¹_d and H²_d, as well as those observed for protons H¹_e and H²_e, coalesce into one signal only in each case (Figure 12b). By employing the approximate coalescence method, the kinetic parameters associated with the degenerate site exchange processes were determined (Table 2).^[13]

Conclusions

Either chiral centers or the elements of planar chirality were introduced into one of the two mechanically interlocked components of three [2]rotaxanes by means of template-directed syntheses. The degenerate site exchange of certain protons in the tetracationic cyclophane components of these [2]rotaxanes was revealed by variable-temperature ¹H-NMR spectroscopy. The local C_{2h}/C₂ symmetries of the elements of planar chirality incorporated into two of the three [2]rotaxanes enabled the unequivocal elucidation of the mechanism associated with the degenerate site-exchange process. It involves (i) the dislodgment of the 1,5-dioxynaphthalene recognition site, incorporated into the center of the dumbbell-shaped component, from the cavity of the tetracationic cyclophane component, (ii) its 180° rotation

Table 2. Kinetic parameters^[a] associated with the degenerate site-exchange processes in the [2]rotaxanes **7** · 4 PF₆, **11** · 4 PF₆, and **12** · 4 PF₆ in solution

[2]Rotaxane	Probe protons ^[b]	$\Delta\nu$ ^[c] [Hz]	k_c ^[d] [s ⁻¹]	T_c ^[e] [K]	ΔG_c^{\ddagger} ^[f] [kcal mol ⁻¹]	Process ^[g]
7 · 4 PF ₆	H _a	156	347	320	15.1	I/II/III
	H _β	63	140	310	15.1	I/II/III
11 · 4 PF ₆	H _γ	34	76	282	14.1	I/II
	H _δ	69	154	298	14.4	I/II
12 · 4 PF ₆	H _δ	54	119	298	14.1	I/II
	H _ε	54	119	298	14.1	I/II

^[a] Determined by variable-temperature ¹H-NMR spectroscopy (400 MHz) in CD₃CN for **7** · 4 PF₆ and **11** · 4 PF₆ and in (CD₃)₂CO for **12** · 4 PF₆. — ^[b] The labels employed to indicate the probe protons H_a, H_γ, H_δ and H_ε are illustrated in Figures 4–6, 8, and 11. The protons H_β are those located in the β-positions, with respect to the nitrogen atoms, on the bipyridinium units. — ^[c] Limiting frequency separation. — ^[d] Rate constant at the coalescence temperature. — ^[e] Coalescence temperature. — ^[f] Free energy barrier at the coalescence temperature. — ^[g] The degenerate site-exchange processes associated with the [2]rotaxanes in solution are illustrated in Figures 4–6.

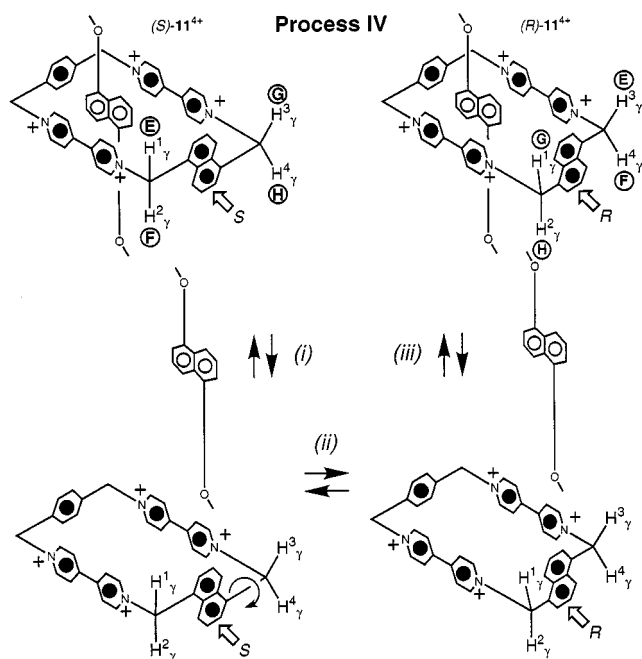


Figure 8. The two enantiomers (*S*) and (*R*) of the [2]rotaxane **11**⁴⁺ and the degenerate site-exchange process IV; E–H indicate the different environments imposed on the methylene protons H¹_γ–H⁴_γ by the local C_{2h} symmetry of the 1,5-dioxynaphthalene ring system and by the local C₂ symmetry of the 1,5-disubstituted naphthalene spacer

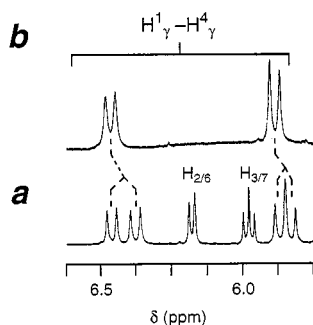


Figure 9. Partial ¹H-NMR spectra of the [2]rotaxane of **11** · 4 PF₆ recorded in CD₃CN at (a) 243 and (b) 304 K; the signals were assigned by two dimensional correlation (COSY) NMR spectroscopy

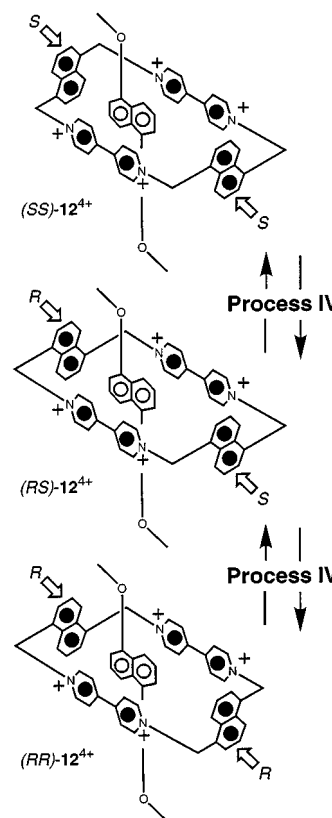


Figure 10. The *meso* form (*RS*) and the two enantiomers (*RR*) and (*SS*) of the [2]rotaxane **12**⁴⁺ and the non-degenerate site-exchange process IV similar to that shown in Figure 5

around the axis of its central carbon–carbon bond or, alternatively, a 180° rotation of the tetracationic cyclophane around an axis passing through its center of inversion and perpendicular to its mean plane, and (iii) the re-insertion of the 1,5-dioxynaphthalene unit inside the cavity of the tetracationic cyclophane component. In addition, variable-temperature ¹H-NMR-spectroscopic investigations have demonstrated that the inversion of the elements of planar chirality embedded within the tetracationic cyclophane components of two of the three [2]rotaxane does not occur on the ¹H-NMR timescale, even at high temperatures. Further understanding of the dynamic processes associated

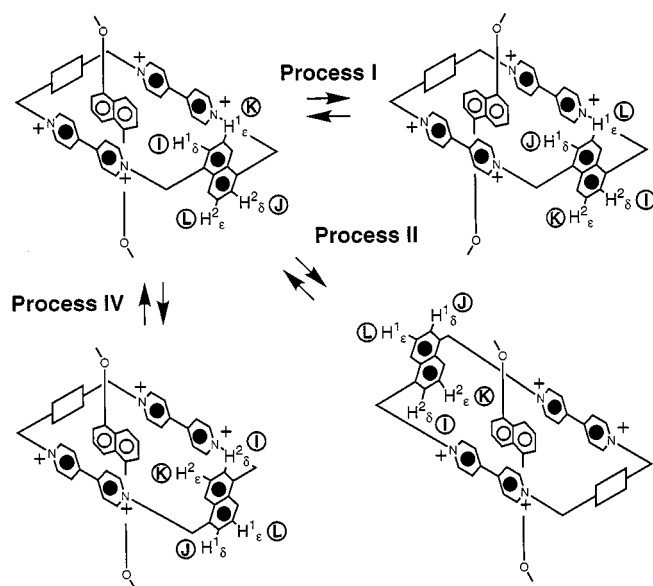


Figure 11. The different environments I–L imposed on the protons H^1_d , H^2_d , H^1_e , and H^2_e by the local C_{2h} symmetry of the 1,5-dioxy-naphthalene unit in the case of the [2]rotaxane 12^{4+} ; processes I and II are similar to those illustrated in Figures 1 and 2, respectively; process IV is similar to the dynamic processes shown in Figures 5 and 7

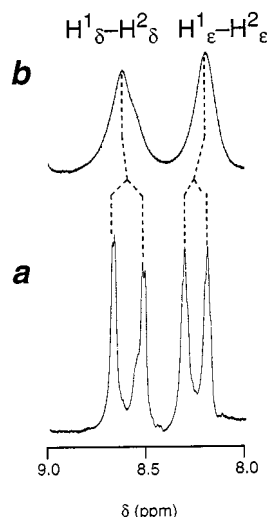


Figure 12. Partial ^1H -NMR spectra of the [2]rotaxane of $12 \cdot 4 \text{PF}_6$ recorded in $(\text{CD}_3)_2\text{CO}$ at (a) 273 and (b) 298 K

with these [2]rotaxanes will be provided by computational studies which are currently in progress in our laboratories.

Experimental Section

General Methods: Chemicals were purchased from Aldrich and used as received. Solvents were dried according to procedures described in the literature.^[16] The compounds **1**,^[17] **5** · 2 PF_6 ,^[18] **8**,^[5] **9** · 2 PF_6 ,^[9] **10**,^[9] **13**,^[19] **15** · 4 PF_6 ,^[1] and **16** · 4 PF_6 ^[9] were prepared according to literature procedures. – Thin layer chromatography (TLC) was carried out using aluminum or plastic sheets precoated with silica gel 60 F (Merck 5554). The plates were inspected by UV light and developed with iodine vapor. Column chromatography was carried out using silica gel 60 F (Merck 9385, 230–400 mesh).

– Melting points were determined with an Electrothermal 9200 apparatus and are not corrected. – Liquid secondary ion mass spectra (LSIMS) were obtained with a VG Zabspec mass spectrometer, equipped with a 35-keV cesium ion gun. Samples were dissolved in either a 3-nitrobenzyl alcohol or 2-nitrophenyl octyl ether matrix, previously coated on to a stainless steel probe tip. – High resolution mass spectra (LSIMS) were obtained with the VG Zabspec operating at a resolution of 6000 and using voltage scanning with CsI as a reference. – ^1H -NMR spectra were recorded with a Bruker AC200 (200 MHz), AC300 (300 MHz), or AMX400 (400 MHz) spectrometer, using either the solvent or TMS as internal standards. – ^{13}C -NMR spectra were recorded with a Bruker AC200 (50.3 MHz), AC300 (75.5 MHz) or AMX400 (100.6 MHz) spectrometer, using either the solvent or TMS as internal standards. All chemical shifts are quoted in ppm on the δ scale and the coupling constants are expressed in Hertz (Hz). – Microanalyses were performed by the University of North London Microanalytical Service or by Quantitative Technologies Inc.

1,5-Bis(2-[2-[1-(*tert*-butoxycarbonyl)methoxy]ethoxy]ethoxy)naphthalene (2): A solution of NaOH (13.6 g, 3.4 mmol) in H_2O (25 mL) was added to a solution of **1** (0.7 g, 2.1 mmol), Bu_4NI (0.7 g, 2.1 mmol) and $\text{BrCH}_2\text{CO}_2\text{tBu}$ (2.4 g, 12 mmol) in CH_2Cl_2 (25 mL). The mixture was stirred vigorously for 7 d before it was diluted with CH_2Cl_2 and H_2O . The solvent was removed under reduced pressure and the residue was purified by column chromatography [SiO_2 : MeCO_2Et /hexane (1:1)] to afford **2** (295 mg, 25%) as a white solid, m.p. 80.9–81.2°C. – LSIMS; m/z : 564 $[\text{M}]^+$. – ^1H NMR (200 MHz, CDCl_3 , 25°C): δ = 7.77 (2 H, d, J = 8 Hz), 7.30–7.17 (2 H, m), 6.71 (2 H, d, J = 8 Hz), 4.20–3.60 (20 H, m), 1.35 (18 H, s). – ^{13}C NMR (50.3 MHz, CDCl_3 , 25°C): δ = 169.6, 154.3, 126.7, 125.0, 114.6, 105.6, 81.4, 70.9, 70.8, 69.8, 69.0, 67.9, 28.0. – $\text{C}_{30}\text{H}_{44}\text{O}_{10} \cdot 0.5 \text{H}_2\text{O}$ (573.7): calcd. C 62.81, H 7.90; found C 62.80, H 7.49.

1,5-Bis(2-[2-[1-(*carboxy*)methoxy]ethoxy]ethoxy)naphthalene (3): A solution of $\text{CF}_3\text{CO}_2\text{H}$ (600 μL , 8 mmol) and **2** (0.29 g, 0.5 mmol) in CH_2Cl_2 (3 mL) was stirred for 12 h at ambient temperature. The solvent was removed under reduced pressure to afford **3** (0.19 g, 82%) as a white solid, m.p. 116°C. – LSIMS; m/z : 452 $[\text{M}]^+$. – ^1H NMR (200 MHz, CDCl_3 , 25°C): δ = 7.78 (2 H, d, J = 8 Hz), 7.46–7.23 (2 H, m), 6.78 (2 H, d, J = 8 Hz), 4.30–3.36 (20 H, m). – ^{13}C NMR (100 MHz, CDCl_3 , 25°C): δ = 172.3, 154.2, 126.8, 125.2, 114.7, 106.0, 71.4, 70.7, 70.0, 68.7, 67.8. – $\text{C}_{22}\text{H}_{28}\text{O}_{10}$ (452.5): calcd. C 58.40, H 6.24; found C 58.03, H 6.13.

1,5-Bis(2-[2-[1-[(1*R*,2*S*,5*R*)-menthoxy]carbonyl]methoxy]ethoxy)naphthalene (4): A suspension of **3** (0.23 g, 0.5 mmol), $(\text{COCl})_2$ (443 μL , 5 mmol), and three drops of DMF in dry CH_2Cl_2 (50 mL) was stirred for 1 d at ambient temperature under N_2 . The solvent was removed under reduced pressure, the residue was dissolved in dry PhMe (20 mL) and (1*R*,2*S*,5*R*)-menthol (238 mg, 1.5 mmol) and $\text{C}_5\text{H}_5\text{N}$ (82 μL , 1 mmol) were added under N_2 . The solution was heated under reflux for 2 d. The solvent was removed under reduced pressure and the residue was purified by column chromatography [SiO_2 : MeCO_2Et / CH_2Cl_2 (1:50)] to afford **4** (79 mg, 21%). – $[\alpha]_{589} = -38$ (c = 0.25 in CH_2Cl_2). – LSIMS; m/z : 728 $[\text{M}]^+$. – HR-LSIMS; m/z : calcd. for $[\text{M}]^+$ ($\text{C}_{42}\text{H}_{64}\text{O}_{10}$) 728.4500; found 728.4502. – ^1H NMR (200 MHz, CDCl_3 , 25°C): δ = 7.80 (2 H, d, J = 8 Hz), 7.33–7.20 (2 H, m), 6.77 (2 H, d, J = 8 Hz), 4.80–4.60 (2 H, m), 4.26–3.53 (20 H, m), 1.60–0.60 (36 H, m). – ^{13}C NMR (75 MHz, CDCl_3 , 25°C): δ = 170.1, 154.3, 126.8, 125.1, 114.7, 105.7, 74.8, 71.0, 69.9, 68.8, 67.9, 46.9, 40.9, 34.2, 31.4, 26.3, 23.4, 22.0, 20.7, 16.3.

[2]Rotaxane 7 · 4 PF_6 : A solution of **4** (45 mg, 0.06 mmol), **5** · 2 PF_6 (129 mg, 0.18 mmol), and **6** (48 mg, 0.18 mmol) in dry MeCN

(3 mL) was stirred for 10 d at ambient temperature. The solvent was removed under reduced pressure and the residue was washed with Et₂O and suspended in Me₂CO. After filtration, the solvent was removed under reduced pressure and the residue was purified by column chromatography [SiO₂: MeOH/2 M NH₄Cl_{aq}/MeNO₂ (7:2:1)] to afford a purple solid. The solid was dissolved in H₂O and NH₄PF₆ was added to the resulting solution to afford a precipitate, which was filtered off and dried to yield **7** · 4 PF₆ (62 mg, 55%) as a purple solid, m.p. > 300°C. – [α]_D²⁰ = –68 (*c* = 0.20 in CH₃CN). – LSIMS; *m/z*: 1683 [M – PF₆]⁺, 1540 [M – 2 PF₆]⁺, 1394 [M – 3 PF₆]⁺. – ¹H NMR (400 MHz, CD₃CN, 25°C): δ = 9.04 (4 H, br. s), 8.64 (4 H, br. s), 8.14–7.90 (8 H, m), 7.41 (4 H, br. s), 7.23 (4 H, br. s), 6.27 (2 H, d, *J* = 8 Hz), 6.12–5.96 (2 H, m), 5.82–5.60 (8 H, m), 4.63–4.57 (2 H, m), 4.35–3.90 (20 H, m), 2.46 (2 H, d, *J* = 8 Hz), 1.80–0.70 (30 H, m), 0.60 (6 H, d, *J* = 7 Hz). – ¹³C NMR (100 MHz, CD₃CN, 25°C): δ = 170.1, 151.0, 145.2, 144.3, 126.6, 128.2, 128.0, 124.4, 114.2, 108.4, 104.3, 74.6, 70.8, 69.8, 68.1, 64.1, 33.7, 31.1, 29.9, 28.7, 26.0, 23.0, 21.2, 19.9, 15.6. – C₇₈H₉₆F₂₄N₄O₁₀P · 0.5 H₂O (1838.5): calcd. C 50.96, H 5.52; found C 50.69, H 5.29. – Single crystals, suitable for X-ray-crystallographic analysis, were grown by vapor diffusion of *i*Pr₂O into an MeCN solution of **7** · 4 PF₆. X-ray data: C₇₈H₉₆N₄O₁₀ · 4 PF₆ · 3.5MeCN, *M* = 1973.2, triclinic, *P*1 (no. 1), *a* = 12.148(1), *b* = 19.212(2), *c* = 21.421(1) Å, α = 108.37(1), β = 94.21(1), γ = 97.33(1)°, *V* = 4671.8(6) Å³, *Z* = 2 (there are two crystallographically independent molecules in the asymmetric unit), *D*_c = 1.403 g cm^{–3}, μ(Cu-Kα) = 16.9 cm^{–1}, *F*(000) = 2050, *T* = 183 K; red platy rhombs, 0.55 × 0.32 × 0.18 mm, Siemens P4/RA diffractometer, ω-scans, 15218 independent reflections. The structure was solved by direct methods and the non-hydrogen atoms refined anisotropically using blocked full-matrix least squares based on *F*² to give *R*₁ = 0.103, *wR*₂ = 0.273 for 12462 independent observed reflections [*I*_o] > 4σ(*I*_o), 2θ ≤ 124°] and 2351 parameters. The absolute structure was unambiguously determined by a combination of *R* factor tests [*R*₁⁺ = 0.1027, *R*₁[–] = 0.1041] and by use of the Flack parameter [*x*⁺ = –0.01(4), *x*[–] = +1.01(4)].^[20]

[2]Rotaxane 11 · 4 PF₆. – Method A: A solution of **5** · 2 PF₆ (220 mg, 0.31 mmol), **8** (78 mg, 0.10 mmol), and **10** (380 g, 1.44 mmol) in dry MeCN (5 mL) was stirred for 15 d at room temp. The solvent was removed under reduced pressure and the residue was washed with Et₂O and suspended in Me₂CO. After filtration, the solvent was removed under reduced pressure and the residue was purified by column chromatography [SiO₂: MeOH/2 M NH₄Cl_{aq}/MeNO₂ (7:2:1)] to afford a purple solid. The solid was dissolved in H₂O and NH₄PF₆ was added to the resulting solution to afford **11** · 4 PF₆ (49 mg, 24%) as a purple solid, m.p. > 300°C. – LSIMS; *m/z*: 1743 [M – PF₆]⁺, 1597 [M – 2 PF₆]⁺, 1452 [M – 3 PF₆]⁺. – ¹H NMR (400 MHz, CD₃CN, 70°C): δ = 8.83–8.75 (10 H, m), 8.31 (2 H, d, *J* = 10 Hz), 8.10–8.06 (2 H, m), 8.20 (4 H, s), 7.26 (8 H, br. s), 6.56 (2 H, d, *J* = 12 Hz), 6.14–6.13 (2 H, br. s), 5.97 (2 H, d, *J* = 12 Hz), 5.78–5.71 (4 H, m), 4.23–3.70 (26 H, m), 2.63 (2 H, d, *J* = 8 Hz), 1.10–0.90 (42 H, m). – C₈₀H₁₀₆F₂₄N₄O₈P₄Si₂ (1887.8): calcd. C 50.86, H 5.66, N 2.97; found C 50.86, H 5.66, N 2.86. – Single crystals, suitable for X-ray crystallographic analysis, were grown by vapor diffusion of *t*BuOMe into a MeCN solution of **11** · 4 PF₆. X-ray data: C₈₀H₁₀₆N₄O₈Si₂ · 4 PF₆, *M* = 1887.8, triclinic, *P*1̄ (no. 2), *a* = 10.829(3), *b* = 12.227(3), *c* = 18.955(6) Å, α = 92.13(3), β = 104.98(3), γ = 110.23(2)°, *V* = 2252.7(11) Å³, *Z* = 1 (the molecule has crystallographic C_i symmetry), *D*_c = 1.392 g cm^{–3}, μ(Cu-Kα) = 19.4 cm^{–1}, *F*(000) = 982, *T* = 203 K; orange plates, 0.60 × 0.37 × 0.10 mm, Siemens P4/RA diffractometer, ω-scans, 6620 independent reflections. The structure was solved by direct methods and the major occupancy non-hydrogen atoms re-

finied anisotropically using full-matrix least squares based on *F*² to give *R*₁ = 0.110, *wR*₂ = 0.291 for 4253 independent observed reflections [*I*_o] > 4σ(*I*_o), 2θ ≤ 120°] and 726 parameters.^[20] – **Method B:** A solution of **6** (110 mg, 0.31 mmol), **8** (86 mg, 0.11 mmol), and **9** · 2 PF₆ (250 mg, 0.31 mmol) in dry MeCN (5 mL) was stirred for 15 d at room temp. The solvent was removed under reduced pressure and the residue was washed with Et₂O and suspended in Me₂CO. After filtration, the solvent was removed under reduced pressure and the residue was purified by column chromatography [SiO₂: MeOH/2 M NH₄Cl_{aq}/MeNO₂ (7:2:1)] to afford a purple solid. The solid was dissolved in H₂O and NH₄PF₆ was added to the resulting solution to afford a precipitate which was filtered off and dried to yield **11** · 4 PF₆ (34 mg, 15%) as a purple solid.

[2]Rotaxane 12 · 4 PF₆: A solution of **8** (17 mg, 0.16 mmol), **9** · 2 PF₆ (320 mg, 0.45 mmol), and **10** (140 mg, 0.45 mmol) in dry MeCN (5 mL) was stirred for 15 d at room temp. The solvent was removed under reduced pressure and the residue was washed with Et₂O and suspended in Me₂CO. After filtration, the solvent was removed under reduced pressure and the residue was purified by column chromatography [SiO₂: MeOH/2 M NH₄Cl_{aq}/MeNO₂ (7:2:1)] to afford a purple solid. The solid was dissolved in H₂O and NH₄PF₆ was added to the resulting solution to afford a precipitate which was filtered off and dried to yield **12** · 4 PF₆ (87 mg, 28%) as a purple solid, m.p. > 300°C. – LSIMS; *m/z*: 1792 [M – PF₆]⁺, 1647 [M – 2 PF₆]⁺, 1502 [M – 3 PF₆]⁺. – HR-LSIMS; *m/z*: calcd. for [M – 2 PF₆]⁺ (C₈₄H₁₀₈F₁₂N₄O₈P₂Si₂) 1646.6989; found 1646.7011. – ¹H NMR (400 MHz, CD₃CN, 70°C): δ = 8.72–8.67 (12 H, m), 8.25 (4 H, d, *J* = 7 Hz), 8.07–7.98 (4 H, m), 7.27–7.08 (8 H, m), 6.50 (2 H, d, *J* = 8 Hz), 5.97–5.82 (8 H, m), 4.18–3.67 (24 H, m), 3.27 (2 H, d, *J* = 8 Hz), 2.66 (0.40 H, d, *J* = 8 Hz), 2.48 (1.6 H, d, *J* = 8 Hz), 1.08–0.95 (42 H, m). – Single crystals, suitable for X-ray crystallographic analysis, were grown by vapor diffusion of *i*Pr₂O into an MeCN solution of **12** · 4 PF₆. X-ray data: C₈₄H₁₀₈N₄O₈Si₂ · 4 PF₆ · 2 H₂O, *M* = 1973.8, monoclinic, *P*2₁/c (no. 14), *a* = 19.840(3), *b* = 12.792(2), *c* = 18.935(2) Å, β = 104.96(1)°, *V* = 4642.8(11) Å³, *Z* = 2 (the molecule has crystallographic C_i symmetry), *D*_c = 1.412 g cm^{–3}, μ(Cu-Kα) = 19.3 cm^{–1}, *F*(000) = 2056, *T* = 183 K; red platy rhombs, 0.67 × 0.37 × 0.07 mm, Siemens P4/RA diffractometer, ω-scans, 6027 independent reflections. The structure was solved by direct methods and the major occupancy non-hydrogen atoms refined anisotropically using full-matrix least squares based on *F*² to give *R*₁ = 0.099, *wR*₂ = 0.253 for 3183 independent observed reflections [*I*_o] > 4σ(*I*_o), 2θ ≤ 120°] and 631 parameters.^[20]

Cyclophane 14 · 4 PF₆: A solution of **5** · 2 PF₆ (220 g, 0.32 mmol), **10** (100 g, 0.32 mmol), and **13** (810 g, 1.58 mmol) in dry MeCN (10 mL) was stirred for 15 d at ambient temperature. The solvent was removed under reduced pressure and the residue was dissolved in H₂O. The aqueous solution was subjected to continuous liquid/liquid extraction with CH₂Cl₂ for 3 d. The aqueous phase was concentrated under reduced pressure and the residue was purified by column chromatography [SiO₂: MeOH/2 M NH₄Cl_{aq}/MeNO₂ (7:2:1)]. The resulting solid was dissolved in H₂O and NH₄PF₆ was added to afford a precipitate which was filtered off and dried to yield **14** · 4 PF₆ (210 g, 56%) as a white solid, m. p. > 300°C. – LSIMS; *m/z*: [M – PF₆]⁺, 860 [M – 2 PF₆]⁺, 715 [M – 3 PF₆]⁺. – ¹H NMR (300 MHz, CD₃CN, 25°C): δ = 8.92 (4 H, d, *J* = 10 Hz), 8.84 (4 H, d, *J* = 7 Hz), 8.36 (2 H, d, *J* = 9 Hz), 8.11–8.06 (8 H, m), 7.95 (2 H, d, *J* = 7 Hz), 7.73–7.67 (2 H, m), 7.49 (4 H, s), 6.57 (2 H, d, *J* = 14 Hz), 5.99 (2 H, d, *J* = 14 Hz), 5.72 (4 H, s). – ¹³C-NMR (75 MHz, CD₃CN, 25°C): δ = 151.0, 151.1, 146.1, 146.0, 136.7, 132.2, 132.0, 131.4, 131.1, 128.6, 128.1, 127.9, 126.3,

65.5, 63.0. — $C_{40}H_{34}F_{24}N_4P_4$ (1150.6): calcd. C 41.76, H 2.97, N 4.87; found C 41.32, H 3.01, N 4.66.

[2]Pseudorotaxane [13:14]·4 PF₆: Single crystals, suitable for X-ray crystallographic analysis, were grown by vapor diffusion of *i*Pr₂O into an equimolar MeCN solution of **13** and **14**·4 PF₆. X-ray data: triclinic, *P* $\bar{1}$ (no. 2), *a* = 14.006(1), *b* = 14.128(1), *c* = 22.632(2) Å, α = 73.94(1), β = 78.53(1), γ = 78.04(1)°, *V* = 4162.0(7) Å³, *T* = 183 K, Siemens P4/RA diffractometer, ω -scans, 10392 independent reflections, 3005 observed reflections [$|F_o| > 4\sigma(|F_o|)$], $2\theta \leq 110^\circ$. The structure was extensively disordered (see text).^[20]

- [1] M. Asakawa, W. Dehaen, G. L'abbé, S. Menzer, J. Nouwen, F. M. Raymo, J. F. Stoddart, D. J. Williams, *J. Org. Chem.* **1996**, *61*, 9591–9595 and references therein.
- [2] For reviews and accounts on template-directed syntheses, see: [2a] D. H. Busch, N. A. Stephenson, *Coord. Chem. Rev.* **1990**, *100*, 119–154. — [2b] J. S. Lindsey, *New J. Chem.* **1991**, *15*, 153–180. — [2c] D. H. Busch, *J. Inclusion Phenom.* **1992**, *12*, 389–395. — [2d] S. Anderson, H. L. Anderson, J. K. M. Sanders, *Acc. Chem. Res.* **1993**, *26*, 469–475. — [2e] R. Cacciapaglia, L. Mandolini, *Chem. Soc. Rev.* **1993**, *22*, 221–231. — [2f] R. Hoss, F. Vögtle, *Angew. Chem. Int. Ed. Engl.* **1994**, *33*, 375–384. — [2g] J. P. Schneider, J. W. Kelly, *Chem. Rev.* **1995**, *95*, 2169–2187. — [2h] D. Philp, J. F. Stoddart, *Angew. Chem. Int. Ed. Engl.* **1996**, *35*, 1155–1196. — [2i] F. M. Raymo, J. F. Stoddart, *Pure Appl. Chem.* **1996**, *68*, 313–322. — [2j] M. C. T. Fyfe, J. F. Stoddart, *Acc. Chem. Res.* **1997**, *30*, 393–401.
- [3] For reviews and accounts on rotaxanes, see: [3a] C. O. Dietrich-Buchecker, J.-P. Sauvage, *Bioorg. Chem. Front.* **1991**, *2*, 195–248. — [3b] J.-C. Chambron, C. O. Dietrich-Buchecker, J.-P. Sauvage, *Top. Curr. Chem.* **1993**, *165*, 131–162. — [3c] H. W. Gibson, H. Marand, *Adv. Mater.* **1993**, *5*, 11–21. — [3d] H. W. Gibson, M. C. Bheda, P. T. Engen, *Prog. Polym. Sci.* **1994**, *19*, 843–945. — [3e] F. Vögtle, T. Dönnwald, T. Schmidt, *Acc. Chem. Res.* **1996**, *29*, 451–460. — [3f] R. Jäger, F. Vögtle, *Angew. Chem. Int. Ed. Engl.* **1997**, *36*, 930–944. — [3g] D. B. Amabilino, J. F. Stoddart, *Chem. Rev.* **1995**, *95*, 2725–2828. — [3h] M. Belohradsky, F. M. Raymo, J. F. Stoddart, *Collect. Czech. Chem. Commun.* **1996**, *61*, 1–43.
- [4] [4a] R. E. Gillard, F. M. Raymo, J. F. Stoddart, *Chem. Eur. J.* **1997**, *3*, 1933–1940. — [4b] F. M. Raymo, J. F. Stoddart, *Chemtracts* **1998**, *11*, 491–511.
- [5] J. A. Bravo, F. M. Raymo, J. F. Stoddart, A. J. P. White, D. J. Williams, *Eur. J. Org. Chem.* **1998**, 2565–2571.
- [6] For a definition of the term “co-conformation”, see: M. C. T. Fyfe, P. T. Glink, S. Menzer, J. F. Stoddart, A. J. P. White, D. J. Williams, *Angew. Chem. Int. Ed. Engl.* **1997**, *36*, 2068–2070.
- [7] For examples of chiral [2]pseudorotaxanes, see: [7a] M. Asakawa, H. M. Janssen, E. W. Meijer, D. Pasini, J. F. Stoddart, *Eur. J. Org. Chem.* **1998**, 983–986. — [7b] M. Asakawa, P. R. Ashton, W. Hayes, H. M. Janssen, E. W. Meijer, S. Menzer, D. Pasini, J. F. Stoddart, A. J. P. White, D. J. Williams, *J. Am. Chem. Soc.* **1998**, *120*, 920–931.
- [8] For examples of chiral [2] rotaxanes, see: [8a] C. Yamamoto, Y. Okamoto, T. Schmidt, R. Jäger, F. Vögtle, *J. Am. Chem. Soc.* **1997**, *119*, 10547–10548. — [8b] A. Archut, W. M. Müller, S. Baumann, M. Habel, F. Vögtle, *Liebigs Ann.* **1997**, 495–499. — [8c] P. R. Ashton, S. R. L. Everitt, M. Gómez-López, N. Jayaraman, J. F. Stoddart, *Tetrahedron Lett.* **1997**, *38*, 5691–5694.
- [9] For examples of [2]catenanes incorporating elements of planar chirality, see: P. R. Ashton, S. E. Boyd, S. Menzer, D. Pasini, F. M. Raymo, N. Spencer, J. F. Stoddart, A. J. P. White, D. J. Williams, P. G. Wyatt, *Chem. Eur. J.* **1998**, *4*, 299–310.
- [10] It is not possible to establish crystallographically the relative populations of the stereoisomers associated with the tetracationic cyclophane component.
- [11] [11a] I. O. Sutherland, *Annu. Rep. NMR Spectrosc.* **1971**, *4*, 71–235. — [11b] J. Sandström, *Dynamic NMR Spectroscopy*, Academic Press, London, **1982**.
- [12] It is not possible to establish by variable-temperature ¹H-NMR spectroscopy if two, or indeed all three, dynamic processes are occurring in solution. As a result, we cannot ascribe the derived energy barrier to any of the three processes uniquely. For related examples, see ref.^[5]
- [13] It is not possible to establish by variable-temperature ¹H-NMR spectroscopy if only one or both processes **I** and **II** are occurring in solution. As a result, we cannot ascribe the derived energy barrier to either process **I** or **II**. For related examples, see ref.^[5]
- [14] For a related example, see ref.^[5]
- [15] Note that the site-exchange processes **I** and **II** are degenerate, while the site-exchange process **IV** is non-degenerate since it interconverts (Figure 10) the achiral and chiral forms of **12**·4 PF₆.
- [16] B. S. Furniss, A. J. Hannaford, P. W. G. Smith, A. R. Tatchell, *Practical Organic Chemistry*, Longman, New York, **1989**.
- [17] P. R. Ashton, A. Chemin, C. G. Claessens, S. Menzer, J. F. Stoddart, A. J. P. White, D. J. Williams, *Eur. J. Org. Chem.* **1998**, 969–981.
- [18] P.-L. Anelli, P. R. Ashton, R. Ballardini, V. Balzani, M. Delgado, M. T. Gandolfi, T. T. Goodnow, A. E. Kaifer, D. Philp, M. Pietraszkiewicz, L. Prodi, M. V. Reddington, A. M. Z. Slawin, N. Spencer, J. F. Stoddart, C. Vicent, D. J. Williams, *J. Am. Chem. Soc.* **1992**, *114*, 198–213.
- [19] P. R. Ashton, J. Huff, S. Menzer, I. W. Parsons, J. A. Preece, J. F. Stoddart, M. S. Tolley, A. J. P. White, D. J. Williams, *Chem. Eur. J.* **1996**, *2*, 31–44.
- [20] Crystallographic data (excluding structure factors) for the structures reported in this paper have been deposited with the Cambridge Crystallographic Data Centre as supplementary publication no. CCDC-108616/108617/108618. Copies of the data can be obtained free of charge on application to CCDC, 12 Union Road, Cambridge CB2 1EZ, UK [Fax: int. code + 44-1223/336-033; E-mail: deposit@ccdc.cam.ac.uk].

Received November 12, 1998

[O98513]